Antiproton-proton charge exchange between 1 and 3 GeV/c*

D. Cutts,† M. L. Good, P. D. Grannis, D. Green,‡ Y. Y. Lee,§ R. Pittman,‖ and J. Storer¶
State University of New York, Stony Brook, New York 11794

A. Benvenuti, G. C. Fischer,** and D. D. Reeder
University of Wisconsin, Madison, Wisconsin 53706

(Received 14 January 1974; revised manuscript received 26 August 1977)

We have measured the reaction cross section for $\bar{p}p \to \bar{n}n$ in small momentum steps between 0.97 and 3.13 Gev/c to a high level of statistical accuracy. Structures are observed in the vicinity of $P_{\text{lab}} = 1.25$ GeV/c and 1.8 GeV/c which are consistent with the structure observed in the $\bar{p}p$ total cross section.

We report here on an experimental study of the reaction $\bar{p}p \to \bar{n}n$ with $\bar{p}$ momenta in the range 0.97 to 3.13 GeV/c. Our scintillation-counter experiment was performed at the Brookhaven Alternating Gradient Synchrotron (AGS) in a partially separated beam. We have measured various features of the charge-exchange scattering, i.e., the reaction cross section σ_R, $d\sigma/dt$ within the t-range $0 \leq |t| \leq 0.1$ (GeV/c)^2, $d\sigma/du$ within the u range $0 \leq |u| \leq 0.06$ (GeV/c)^2, and the differential cross section near c.m. angle $\theta^* = 90°$. This paper discusses the experimental method and gives results for σ_R.

Antiproton charge exchange is interesting for several reasons. The t-channel quantum numbers allow the exchange of charged, nonstrange mesons, free from diffractive effects; in particular, the reaction permits the study of π exchange. The u-channel states have $B = 2$, $Q = 1$ and are generally expected to give small contributions to the cross section. The s-channel states include all nonstrange mesons ($m \geq 2M_N$). Various experiments have been directed at the production of high-mass mesons in πp collisions[1]; evidence from $\bar{p}p$ total-cross-section measurements[2] indicates the presence of some small s-dependent structures although their interpretation as resonances is not clear due to possible inelastic threshold effects.[3] The expected picture then for $\bar{p}p$ charge exchange is that resonance or s-channel effects give rise to amplitudes symmetric or antisymmetric about $\theta_{\text{c.m.}} = 90°$ with t-channel exchanges adding strong forward peaked amplitudes and u-channel exchanges contributing weakly to a backward amplitude. This picture is qualitatively borne out by our observation that the backward cross section varies between about 2% and 1% of the forward cross section from 1 to 3 GeV/c.[4] The reaction cross section σ_R is the integral of the differential cross section and thus can be used to elucidate the s dependences, complementary to σ_T measurements.

Our experiments was performed in the partially separated beam of antiprotons from the G-10 target of the AGS. The general experimental arrangement is shown in Fig. 1. At the lower momenta (less than 2 GeV/c), the measured time of flight between beam counters T_1 and T_2 (separated by 105 feet) was sufficient to separate $\bar{\pi}$ and $\bar{p}$. At higher momenta, pions were rejected by a Freon Čerenkov counter $\check{C}$, in the beam. The momentum acceptance of the beam was about ±3%; for a fraction of the events, the beam momentum was measured to ±1/4% with a system of proportional wire

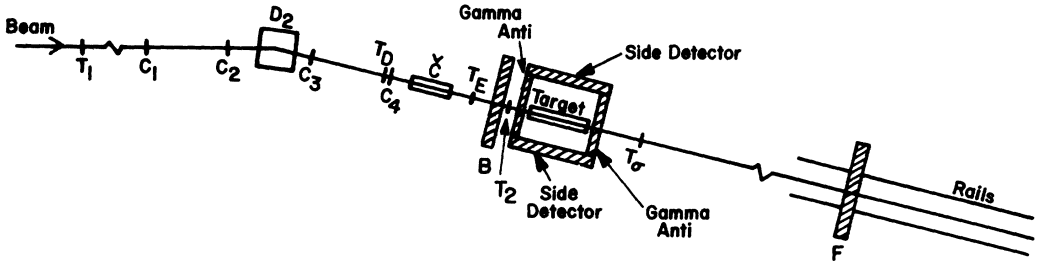

FIG. 1. Schematic layout of the experiment. Scintillators T_1, T_E, and T_2 define the incident $\bar{p}$ beam; proportional wire chambers C_1, C_2, C_3, C_4 measure the horizontal beam coordinate before and after bending magnet D_2. The Freon threshold Čerenkov counter $\check{C}$ detects π's, and scintillator T_D monitored extra beam particles in close time proximity with an event. The downstream detector F is movable along the beam direction.

chambers C_1–C_4 before and after the last bending magnet. Runs were taken at about 40 different beam momenta separated from each other by an amount equal to the beam momentum spread (3%).

The liquid hydrogen target consisted of three 12-inch long cylindrical segments separated by $\frac{1}{2}$ inch. Counters T_3 and T_4 placed in these gaps provided some localization of the interaction vertex. The target was surrounded by a box of nine veto counters A_C^i, with a hole for the beam entrance. The logical "or" of the nine A_C^i counters is referred to as A_C: $A_C = \sum_{i=1}^{9} A_C^i$. Outside the A_C box there were γ-detecting arrays of scintillator and heavy metal. These γ detectors were separated into two groups: 32 lead-scintillator counters A_γ, above, below, upstream, and downstream of the target; and steel-scintillator arrays S, to either side of the target. These two arrays were used to detect the γ's from π^0's produced in $\bar{p}p$ collisions and together completely filled the solid angle around the target, except for a small beam-entrance hole. In addition to the γ veto function, the array S was used in the differential cross-section measurements to detect and identify the slow n or $\bar{n}$ emitted near 180° in the c.m. (and hence near 90° laboratory angle). For $t < 0.1$ GeV^2 the neutron has an angle of $\theta_n > 68°$ relative to the beam direction, and a time of flight from target to S (or A_γ) greater than 10 nsec. The arrangement of detectors in the target region is shown in Fig. 2.

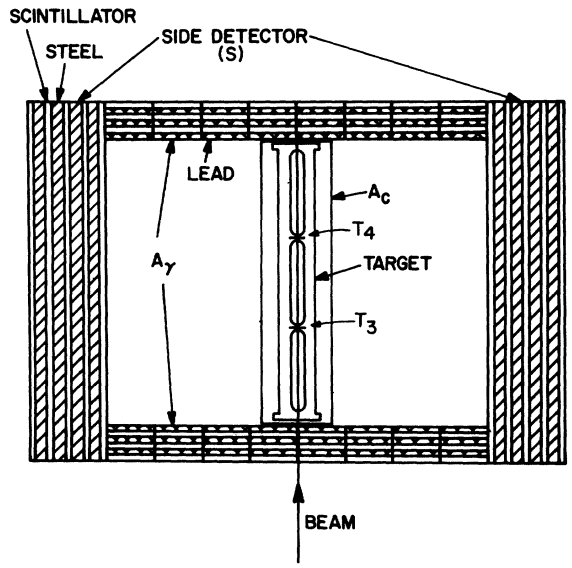

FIG. 2. Arrangement of counter hodoscopes around the hydrogen target (top view). A portion of the lead-scintillator A_γ is shown together with the side detector S. The charged-veto box A_C surrounds the target with the exception of a small beam-entrance hole. There is also a beam-entrance hole in A_γ.

A hodoscope F of six alternating layers of iron and scintillator slats, permitting x-y definition to within a four-inch square, was located on the beam axis downstream of the target. The F hodoscope was movable and was used to detect the $\bar{n}$ or n emitted near 0° in the c.m. in the differential cross-section measurements. In normal operation, this hodoscope was positioned so as to subtend a fixed region of t. A similar hodoscope B was located upstream of the target and was used in a search for $\bar{p}p \to K_L^0 K_L^0$. Finally, there was a counter T_σ on the beam axis, which was used to monitor the transmission of $\bar{p}$ through the hydrogen, A_C, and A_γ detectors.

The trigger was logically the requirement of a beam $\bar{p}$ incident on the target with no charged particles emerging: trigger $= T_1 \cdot T_2 \cdot T_E \cdot \bar{C} \cdot \bar{A}_C$. For every trigger each element of the A_γ, S, F, and B arrays which gave a count was recorded, together with its pulse-area and the time of the recorded relative to beam counter T_2. Also recorded were the proportional wire chamber coordinates, the status of the counters T_3, T_4 in the gaps of the target, and tag bits indicating the presence of extra beam particles in time proximity which could have confused the analysis. From the status of T_3 and T_4 in each event, the interaction point could be localized to be within one of the 12-inch target segments.

A PDP-8 on-line computer collected these data and transmitted them to magnetic tape as well as to the on-line-data-facility PDP-6 for various checks of the experiment. The most important of the on-line checks were tests of all counter gains by means of computer controlled light diodes attached to each scintillator, monitoring of the counting rates of various trigger categories, checks of the times-of-flight and pulse height for various hodoscopes, measurement of beam profiles, and computation of the ratio $T_1 T_2 T_E \bar{C} T_\sigma / (T_1 T_2 T_E \bar{C})$ giving the fraction of incident beam transmitted. This check was made over intervals of a few minutes to check the stability of liquid hydrogen in the target and allowed later rejection of data taken when bubbling had occurred.

Selection of the event sample for further analysis was made from the trigger sample through several requirements. Tag bits registering the A_C counter bits were interrogated to guard against electronic losses of efficiency in rejecting charged final states. Events which were accompanied by a second beam track within 80 nsec following the triggering $\bar{p}$ were tagged and rejected. Events in which the recorded bits for the interleaved target counters did not permit the establishment of an interaction point were deleted. The times-of-flight recorded for the incident-beam particle were re-

quired to be consistent with that for incident $\bar{p}$. We have also rejected a small fraction of events in which the encoding of struck counters was inconsistent; this effect has been traced to the presence of electrical noise in the experimental hall and was independent of trigger topology. Finally groups of events recorded during times of anomalous beam transmission were rejected. This last cut was made by first calculating the average transmission over a run and deleting any record (of typically 100 events) for which the transmission deviated from the average by more than two standard deviations. The fraction of events rejected by all of these effects was typically 5–10%. Runs for which the combined loss was greater than 10% were omitted in analysis.

The analysis for obtaining charge-exchange events consisted of isolating those events among the selected triggers in which there were no π^0's present. We here assume that the all neutral events satisfying the trigger requirement are either $\bar{p}p \to \bar{n}n$, $\bar{p}p \to \bar{n}n + m\pi^0$, or $\bar{p}p \to m\pi^0$ (we have independently verified that the $\bar{p}p \to K_L^0 K_L^0$ rate is negligibly small).[5] Thus we must eliminate all events showing a γ in any of the A_γ or S hodoscope elements. Since the A_γ array contained 3.6 radiation lengths of lead and S contained 5.7 radiation lengths of iron, we expect an inefficiency for a single γ of about 2.5% for γ energy greater than 50 MeV. We have measured the inefficiency of the γ-veto arrays for events of the type $\pi^- p \to$ neutral, at several momenta, and find that it is less than 2%. To relate this to the inefficiency for $\bar{p}p \to m\pi^0$ and $\bar{p}p \to \bar{n}n + m\pi^0$, one needs some information about γ multiplicities. The mean number of γ's in $\pi^- p \to$ neutrals may be evaluated from existing data compilations. Doing this we find $n_\gamma(\pi p) = 3$, 4, and $4\frac{1}{2}$ at $p_\pi = 1$, 2, and 3 GeV/c, respectively. For $\bar{p}p \to$ neutrals, such data do not exist, so we have taken our own γ-veto multiplicity distribution as a rough guide, obtaining a multiplicity $n_\gamma(\bar{p}p) = 5$ at 1.4 GeV/c and 3.4 at 3 GeV/c. Not all of these events are γ's. A contamination of $\bar{n}$ interactions exists, an upper limit to which can be estimated from the geometric $\bar{n}$ cross section in the forward A_γ shield. This check gives a maximum contamination of 26% at 1.4 GeV/c and 12% at 3 GeV/c. On any reasonable assumption for the multiplicity of the $\bar{n}$ interactions, it is difficult to get the value of $n_\gamma(\bar{p}p)$ below three, at any beam momentum. Thus the γ-veto array inefficiencies which we measured for pions at 1.0 and 1.5 GeV/c [where $n_\gamma(\pi p) \simeq 3$] are relevant. These values are $\leq 1.7\%$ and $\leq 1.5\%$, respectively, and lead to the conclusion that an upper limit to the inefficiency for $\bar{p}p \to \gamma$'s is 2%, at all momenta. Finally, since the charge exchange is half or more of the total neutral cross section, we have an upper limit of 2% contamination of non-charge-exchange events in our sample (see also Ref. 6).

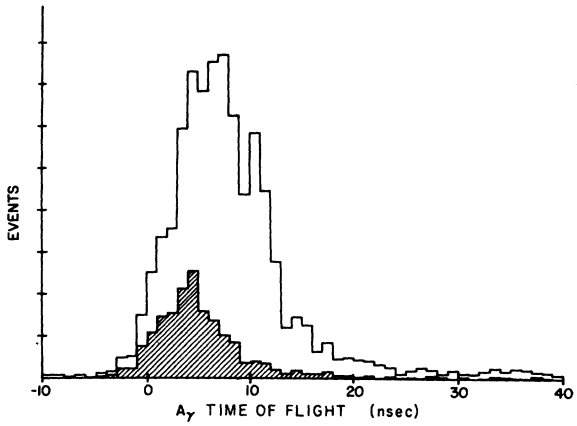

FIG. 3. Time-of-flight distribution for the sum of A_γ counters relative to the beam-defining counter T_2 for the middle target segment at 1.49 GeV/c. The unshaded histogram is for all triggers of the apparatus. The shaded histogram is for that subsample of triggers in which a γ was seen in S.

The typical distribution of γ time of flight between the sum of counters A_γ and the beam-time-defining counter T_2 is shown in Fig. 3. Also shown in Fig. 3 is the sample of events in which we have ensured that there were π^0's produced by requiring in addition an element of the S array to be struck in good time coincidence with the beam. The time-of-flight distribution for γ's in the S array was monitored in the corresponding way by requiring the presence of a γ in A_γ. For both S and A_γ, the cut imposed on the time-of-flight distributions to eliminate events with γ's was 10 nsec later than the most probable time. Such a cut eliminated essentially all such γ events. However, it also eliminated those $\bar{p}p \to \bar{n}n$ events in which a fast $\bar{n}$ or n interacted in A_γ or S and thus a correction must be applied. The location of the most probable γ interaction times in A_γ and S was obtained for each target segment in each separate run; the determination of these cuts was made to ±0.2 nsec corresponding to an uncertainty in event rate of ±0.25%.

Several corrections must be made to the raw sample of events to extract the cross section. We start with the target-empty subtraction. Target-empty data were taken for roughly half the data points, smoothly distributed throughout the momentum range. Target-empty charge-exchange counting rates ranged from 6% to 9% of target full. (A 1.9% effect is expected because of the H_2 vapor filling the nominally empty target.) A smooth curve drawn through the target-empty points was subtracted from the target-full data points. The

result, multiplied by 1.019 to correct the H_2-vapor effect, is the input to the reaction cross-section determination. The statistical error on the background points was typically 10% (of the background), and hence less than 1% of σ_R.

The dominant remaining corrections to the data derive from the attenuation of incident $\bar{p}$ flux in the target and the possibility of $\bar{n}$ interactions. The former can be evaluated from the known $\bar{p}p$ total cross section[2]; the latter comes mainly from forward charge-exchange events since at all energies the cross section is very strongly peaked toward 0°. Thus the forward $\bar{n}$ may interact in the hydrogen or A_C, nullifying the trigger by producing charged secondaries, or it may interact in A_γ giving a γ signature. The combination of these two corrections amounts to the transmission of an antinucleon through the entire fixed portion of the apparatus, the target A_C, and the forward wall of A_γ We argue that this correction cannot be very different from the transmission of beam $\bar{p}$'s through the target A_C, and the forward wall of A_γ, as continuously monitored by the transmission counter T_o, and that it can be fairly well estimated by a simple total-attenuation calculation using known cross sections. Such a calculation agrees with the measured $\bar{p}$ transmission at all momenta, to within a few percent.

In addition, the slow n, near 90° in the laboratory, can interact to produce a count in A_C nullifying the trigger, or to give a signal in the nonforward parts of A_γ or in S. An A_γ or S interaction causes event failure only when the n time-of-flight is in the γ-cut region ($t \geq 0.1$ GeV^2). The neutron corrections are a function of the four-momentum transfer t, but are independent of s since the neutron energy and angle depend only on t.

For $t \lesssim 0.1$ GeV^2 ($E_{\text{neutron}} < 50$ MeV), we have a direct measure of the detection efficiency of S for neutrons, based on events in which a forward $\bar{n}$ was detected in F and the predicted accompanying neutron was looked for in S at the appropriate time delay. This gives a value of 7% for neutron efficiency in S, averaged over the neutron spectrum for $t < 0.1$ GeV^2. For higher values of t, where a correction must be made, the neutron-detection efficiency of the scintillator falls, while the probability of proton recoils being produced in the iron or lead and entering the scintillator increases. The net calculated efficiency for A_γ and S averaged over the angular distribution for $\bar{p}p \to \bar{n}n$, never exceeds 5%. A measured neutron efficiency for a similar detector, namely, the F hodoscope is available from our 180° cross-section measurements.[4] Averaged over the neutron momenta between 1 and 3 GeV/c, it is 20%. In the much lower-energy region represented by the recoil neutrons, it is clearly always much smaller.

There is a further correction due to the escape of beam particles through the sides of the target caused by multiple scattering in $\check{C}$ and other beam counters, and by the finite angular spread of the beam. This effect was measured in target-empty runs and agreed with calculations based on the known beam conditions. We have also determined that the probability of losing a trigger due to the incident $\bar{p}$ producing a δ ray which penetrates to the charge-veto A_C is negligible. Finally, we have measured that there is no discernible effect on our results due to a splashback of charged particles from $\bar{n}$ annihilation in the F hodoscope, even at low energies where F is close to the interaction region.

The corrections discussed here for $\bar{p}$ attenuation, $\bar{n}$ and n interactions, and loss of $\bar{p}$'s through the target sidewalls have been evaluated in a detailed Monte-Carlo calculation. Measured beam parameters and detector geometry are used as input, together with known $\bar{N}N$ cross sections from hydrogen and heavy materials,[7] and angular distributions for $\bar{p}p$ charge exchange taken from our data. The results of this calculation give the factor by which the number of observed charge-exchange events must be multiplied to give the true number. This factor is about 2 and is dominated by the $\bar{p}$ attenuation and $\bar{n}$ interaction corrections. Various checks of the Monte-Carlo calculation can be made with the data to verify its validity. In particular, we have made a simplified analysis of the data based on hand calculations, and compared it to the complete Monte Carlo–corrected results as a check. The simplified analysis took the combined $\bar{p}$-attenuation and $\bar{n}$-interaction corrections to be the same as the measured $\bar{p}$ transmission, and ignored neutron interactions. Corrections for side losses from the target were made using the target-empty T_3 and T_4 data, and a target-empty background subtraction was performed. The result of this simplified calculation is a σ_R value higher than that of the full Monte Carlo calculation by a smoothly varying factor ranging from 3% at 3 GeV/c to 6% at 1 GeV/c. The deviation of this simple calculation from the full calculation is understandable entirely in terms of the effects neglected in the simple version and their energy dependence, as follows:

The simple calculation overestimates the $\bar{n}$-interaction correction, since it assumes that the $\bar{n}$'s traverse the entire remaining length of the target from their point of production, whereas in fact some of them exit the target through the sides, especially at lower beam momenta. It also makes no correction for neutron interactions, which are expected to be an effect of about 10%, and nearly independent of beam momentum. The two effects

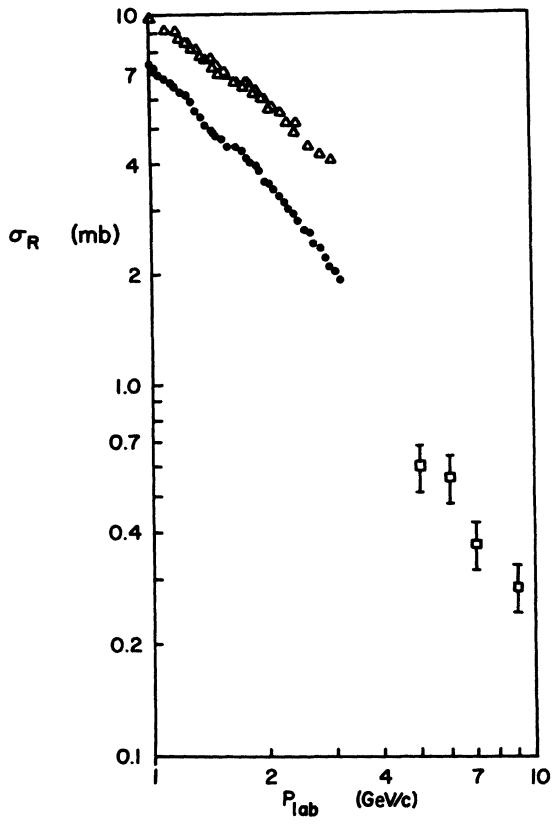

FIG. 4. Reaction cross section σ_R for $\bar{p}p \to \bar{n}n$ versus laboratory momentum. •, data from this experiment; △, data from Bricman *et al.*, Ref. 8; □, data from Astbury *et al.*, Ref. 10.

tend to cancel. Thus the simple calculation nearly agrees with the full one at high momentum, but gives a result noticeably too high at low momenta.

Both of the effects discussed here are included in the full calculation. We feel that the near agreement with the simplified calculation is a reassuring check of the overall validity of the Monte Carlo–corrected results. In addition, we have checked the constancy of σ_R computed for each target segment individually, and compared the calculated sidewall loss of $\bar{p}$ flux for target empty with the observed distribution. A further check involved the extraction of the total cross section σ_T for $\bar{p}p$ from our data. The counter T_σ, downstream of the target and A_γ, was used as a transmission monitor, as mentioned previously. Comparing the transmission ratio for target full and empty, we can compute σ_T. Our results agree with the previous precision measurement[2] to within ±2%.

From all of these checks we conclude that the effects of beam attenuation and $\bar{n}$ and n interactions have been well understood, and attach an overall systematic error of ±10% to the final data. This systematic error applies to the entire set of data between 0.97 and 3.13 GeV/c as a whole. The overall correction to the event rate obtained from the Monte Carlo was obtained at several momenta throughout our momentum range and was applied as a smooth energy-dependent factor. It is found to be variable in magnitude by less than ±10% between 1 and 3 GeV/c.

In addition, using measured accidental rates, we correct for accidental counts in the A_C array which would nullify a trigger, or in the A_γ array within the time region of the γ's (total correction 2–10%). Finally, small overall corrections are applied for the γ inefficiency and for the loss of events (about 2%) in the electronics due to spurious bits set in the logic.

The resulting reaction cross section σ_R for $\bar{p}p \to \bar{n}n$ is shown in Fig. 4. In Fig. 5 we plot $\sigma_R P_{lab}$ to compensate for some of the monotonic decrease in cross section with momentum. The errors shown include statistical errors, our determination of the systematic point-to-point uncertainties, and the energy-dependent Monte Carlo errors. The systematic effects can be due to variations in the beam conditions as well as changes in the exact location of the time zero, relative to which the γ cut was made. Our estimate of the systematic component of error is based on repeated measurement of the cross section at a given momentum within the three-month interval of the experiment. The numerical values for σ_R are given in Table I.

In Fig. 4 we show, in addition to our results, the measured charge-exchange cross sections from other experiments. We note in particular a discrepancy between our results and the previous high-statisctics experiment[8] which is outside the quoted systematic errors of the two experiments. We have discussed above the various checks per-

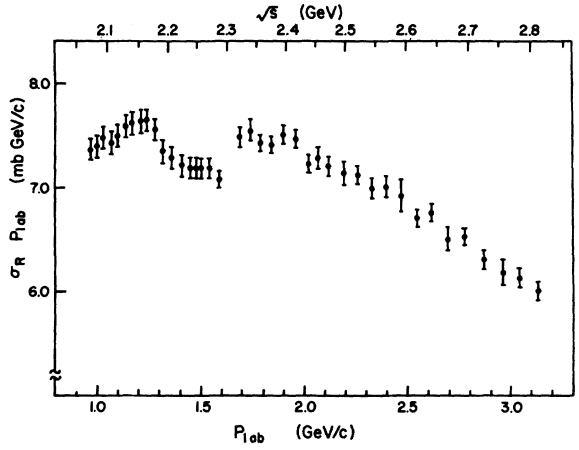

FIG. 5. Reaction cross section for $\bar{p}p \to \bar{n}n$ times laboratory momentum versus laboratory momentum.

TABLE I. Reaction cross section for $\bar{p}p \to \bar{n}n$.

P_{lab} (GeV/c)	$\sqrt{s}$ (GeV)	σ_R (mb)	P_{lab} (GeV/c)	$\sqrt{s}$ (GeV)	σ_R (mb)
0.97	2.072	7.60±0.10	1.79	2.356	4.15±0.04
1.00	2.082	7.40±0.10	1.84	2.374	4.03±0.04
1.03	2.092	7.26±0.10	1.90	2.395	3.95±0.04
1.07	2.105	6.94±0.09	1.96	2.416	3.81±0.04
1.10	2.115	6.82±0.09	2.02	2.437	3.58±0.04
1.14	2.129	6.66±0.09	2.07	2.455	3.52±0.05
1.17	2.139	6.51±0.09	2.12	2.472	3.40±0.04
1.21	2.153	6.31±0.09	2.19	2.496	3.26±0.05
1.24	2.163	6.17±0.08	2.26	2.520	3.15±0.03
1.28	2.177	5.91±0.08	2.33	2.544	3.00±0.04
1.32	2.191	5.57±0.08	2.40	2.568	2.92±0.04
1.36	2.205	5.36±0.07	2.47	2.592	2.80±0.06
1.41	2.222	5.11±0.07	2.55	2.619	2.63±0.03
1.45	2.236	4.96±0.07	2.62	2.643	2.58±0.03
1.48	2.247	4.86±0.07	2.70	2.669	2.41±0.04
1.50	2.254	4.79±0.06	2.78	2.696	2.35±0.03
1.54	2.268	4.67±0.06	2.87	2.725	2.20±0.03
1.59	2.286	4.45±0.05	2.96	2.755	2.09±0.04
1.69	2.321	4.43±0.05	3.04	2.780	2.02±0.03
1.74	2.339	4.34±0.05	3.13	2.809	1.92±0.03

formed on our data to verify the normalizing factors. We suggest that a possible explanation of the discrepancy lies in an overestimate of the number of interacting $\bar{n}$'s in Ref. 8. Indirect evidence supporting our results comes from noting that the sums of the cross sections for $\bar{p}p \to \bar{n}n$, $\bar{p}p \to \bar{n}n + m\pi^0$, and $\bar{p}p \to m\pi^0$ should give the total $\bar{p}p \to$ neutral-final-state cross section.[9,10] Our results allow this sum rule to be satisfied, whereas the results of Ref. 8 are themselves greater than the total neutral cross section. Finally we note that our results extrapolate smoothly to the data above 5 GeV/c.[11]

We note that our results show departures from smooth energy-dependent behavior at two momenta. These structures occur at approximately 1.25 GeV/c and 1.8 GeV/c and have a large width. We find no evidence for any narrow bumps in σ_R within our mass resolution (variable between 10 MeV/c^2 and 30 MeV/c^2 in our momentum range). The structures observed are similar in position and width to those found[2] in $\sigma_T(\bar{p}p)$ and also in a study of $\bar{p}p$ annihilations.[12] These structures have been interpreted, though not uniquely, as s-channel resonances: $I=1$ states at $M=2190$ MeV/c^2 and $M=2345$ MeV/c^2, and an $I=0$ state at $M=2380$ MeV/c^2. The width of these structures is large, incompatible with the narrow structures observed in the previous missing mass results.[13] The enhancements observed in the present data differ somewhat from those reported.[2,12] In the case of the U-region bumps ($M=2360$ MeV/c^2) our experiment does not distinguish between the $I=1$ and $I=0$ cross sections and thus provides a picture of the two states combined. For the T region enhancement ($M \approx 2190$ MeV/c^2) we observe the peak in σ_R at a mass about 40 MeV/c^2 below that reported in previous experiments. Such a difference need not be significant, however, since interference effects between a resonating amplitude and background in the same partial waves can result in a shift in the apparent peak position in σ_R but not in σ_T.

It is of interest to distinguish whether the bumps seen in σ_T and σ_R are resonant effects or are due to another mechanism such as threshold effects associated with opening of new channels [e.g., the $\bar{N}$(1236) threshold occurs near the T bump and the $\bar{N}N^*$ (1400) is near the U bump]. If we assume that the s-dependent bump structure is due to some particular partial-wave amplitude (and take for simplicity the spin singlet amplitude), then the structure observed in σ_T and σ_R can be written as follows:

$$\Delta\sigma_T(\text{pure I}) = 2\Delta\sigma_T(\bar{p}p) = \frac{\pi}{k^2}(2J+1)\,\mathrm{Im}(a_J^s)$$

$$\Delta\sigma_R(\bar{p}p \to \bar{n}n) = \frac{\pi}{k^2}\frac{(2J+1)}{4}\left[2\,\mathrm{Re}(a_J^{B*}a_J^s) + |a_J^s|^2\right],$$

where k = c.m. momentum, and a_J^B and a_J^s are the partial-wave amplitudes for angular momentum J for the s-independent background and the s-dependent structure. These expressions are not materially altered if the triplet amplitudes are the rel-

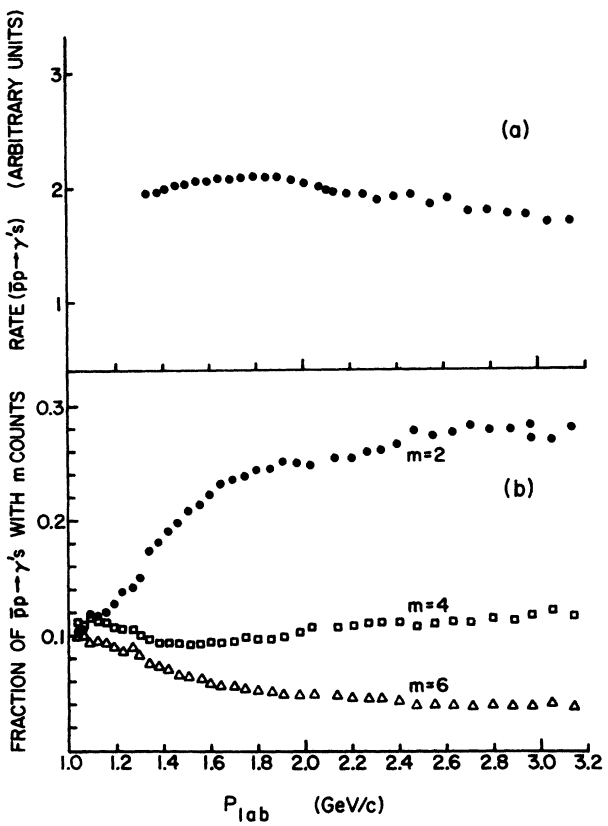

FIG. 6. (a) Rate for the process $\bar{p}p \to \gamma$'s versus laboratory momentum. The normalization is arbitrary. Changes in the experimental arrangement preclude presentation of data below 1.3 GeV/c. (b) Fraction of events showing m participating γ counters versus laboratory momentum: •, $m=2$; □, $m=4$; △, $m=6$.

evant ones.[14] Thus measurement of $\Delta\sigma_T$ and $\Delta\sigma_R$ allow some restrictions to be placed on the effective angular momentum state responsible for the bump. Since we expect a threshold mechanism to contribute to the lowest partial waves, determination of J may help distinguish the resonance versus threshold possibilities.

If we assume no background in the channel J, then the determination of J is straightforward and we find under this hypothesis, effective spins of the T and U structures of about 2 and 4.5, respectively. However, in the more likely case that there is background in partial wave J (as indicated by the difference in the enhancement mass value seen in σ_T and σ_R), the determination of J becomes less reliable and no clear conclusion on the character of the bumps can be made.

Due to the large fraction of the σ_T bump seen in annihilations (and the apparent small coupling to $\bar{N}N$), it is reasonable to search for structure for the class of reactions $\bar{p}p \to m\gamma$. For this study, we have examined the cross sections of those events satisfying the neutral trigger requirement discussed above and which contain m counts in the A_γ and S arrays for which the measured time-of-flight is within the "prompt-γ" cut described previously. The value of m (=number of counters registering a particle) is related to, but not identical with, the γ multiplicity of the event. The nonequality arises due to the possibility of several γ's striking the same counter, effects of shower spreading and "backsplash", and the small but nonzero γ inefficiency of the system. Thus we choose to present our results for the γ events in terms of a rate whose normalization is arbitrary and focus our attention on the s dependence and the dependence on m. The fractional rates for several values of m are shown in Fig. 6 as well as the rate for any number of γ's detected, and these rates show no evidence for structure. The rate for 2γ production rises, in accordance with the opening of the π^0 production channels. We do not feel that the absence of structure in these reactions is surprising, since our trigger has insisted that no charged particles be produced. High mass states decaying directly into many pions have a low probability for producing an all neutral final state due to the Clebsch-Gordan coefficients. Moreover, if the decays of the presumed high-mass state were a cascade process resulting, after several steps of the series, in ρ or A_2 mesons, we would expect essentially no purely π^0 final states.

Thomas Regan and John Moeser have been instrumental in making this experiment successful. Herman Hagerty provided valuable assistance in assembling the apparatus. We would also like to acknowledge the contributions of Glenn Laguna, Stuart Zweben, and Alex Grillo to the running and analysis of this experiment. The AGS staff, under the direction of Dr. David Berley and Tom Blair, has been most helpful.

---

*Research sponsored in part by the U.S. Atomic Energy Commission and National Science Foundation.

†Present address: Department of Physics, Brown University, Providence, Rhode Island 02912.

‡Present address: Department of Physics, Carnegie-Mellon University, Pittsburgh, Pennsylvania 15213.

§Present address: Accelerator Department, Brookhaven National Laboratory, Upton, New York 11973.

‖Present address: Department of Physiology, Medical College of Virginia, Richmond, Virginia 23298.

¶Present address: 307 University Avenue, Davis, California 95616.

**Present address: Rothbury, Michigan 49452.

[1]G. Chikovani, L. Dubal, M. N. Focacci, W. Kienzle, B. Levrat, B. C. Maglic, M. Martin, C. Nef, P. Schubelin, and J. Sguinot, Phys. Lett. 22, 233 (1966); M. N. Focacci, W. Kienzle, B. Levrat, B. C. Maglic, and M. Martin, Phys. Rev. Lett. 17, 890 (1966); Y. M. Antipov, R. Band, R. Busnello, G. Damgaard, M. N. Kienzle-Focacci, W. Kienzle, R. Klanner, L. G. Landsberg, A. A. Lebedev, C. Lechanoine, P. Lecomte, M. Martin, V. Roinishvili, R. D. Sard, F. A. Yotch, and A. Weitsch, Phys. Lett. 40B, 147 (1972); D. Bowen, D. Earles, W. Faissler, D. Garelick, M. Gettner, M. Glaubman, B. Gottschalk, G. Lutz, J. Morimisato, E. I. Shibata, Y. W. Tang, E. Von Goeler, R. Weinstein, H. R. Blieden, G. Finocchiaro, J. Kirz, and R. Thun, Phys. Rev. Lett. 30, 333 (1973). See also the comments on these experiments by W. Kienzle, Phys. Rev. D 7, 3520 (1973).

[2]R. J. Abrams, R. L. Cool, G. Giacomelli, T. F. Kycia, B. A. Leontic, K. K. Li, and D. N. Michael, Phys. Rev. D 1, 1917 (1970).

[3]Accurate data on the p-p total cross section in which the observed structure in the region $P_{\text{lab}}=1.0$–1.5 GeV/c is ascribed to the [$p\Delta(1236)$] threshold is reported by D. V. Bugg, D. C. Salter, G. H. Stafford, R. F. George, K. F. Riley, and R. J. Tapper, Phys. Rev. 146, 980 (1966).

[4]J. Storer, D. Cutts, M. L. Good, P. D. Grannis, D. Green, Y. Y. Lee, R. Pittman, A. Benvenuti, G. C. Fischer, and D. D. Reeder, Phys. Rev. Lett. 32, 950 (1974).

[5]Verification of the small $\bar{p}p\to K_L^0 K_L^0$ cross section has been made up to 1.5 GeV/c by R. R. Burns, P. E. Condon, J. Donahue, M. Mandelkern, L. R. Price, and J. Schultz, Phys. Rev. D8, 1286 (1973); 12, 644 (1975).

[6]Another very conservative upper limit of our γ inefficiency for $\bar{p}p\to$ neutrals may be established as follows: At 1.0 and 1.5 GeV/c, at least 30% of $\pi^- + p\to$ neutrals is the charge-exchange reaction, which gives one π^0, or two γ's. If we blame the measured inefficiency of $<1.6\%$ (see text) entirely on the one π^0 events, we obtain a $\leq 5\%$ inefficiency for such events. Then since at least one π^0 is produced in $\bar{p}p\to m\pi^0$ and $\bar{p}p\to\bar{n}n+m\pi^0$, we have a solid upper limit of 5% for the inefficiency of $\bar{p}p$ events independent of any estimate of their γ multiplicity. We feel the true limit is less than this since (i) more than two γ's are produced, on the average (see text), and (ii) any measurement of γ inefficiencies is always in the form of an upper limit since a few bad triggers can cause the apparently missed γ's. However, this limit is valuable insurance against gross error.

[7]We have used in these calculations $\bar{N}N$ cross sections from Ref. 2 and NN cross sections from Ref. 3. The corresponding N and $\bar{N}$ cross sections for heavy nuclei have been taken from R. J. Abrams, R. L. Cool, G. Giacomelli, T. F. Kycia, B. A. Leontic, K. K. Li, A. Lundby, D. N. Michael, and J. Teiger, Phys. Rev. D 4, 3235 (1971).

[8]C. Bricman, M. Ferro-Luzzi, J. M. Perreau, J. K. Walker, G. Bizard, Y. Declais, J. Duchon, J. Seguinot, and G. Valladas, Phys. Lett. 29B, 451 (1969).

[9]The data for the reactions $\bar{N}N\to\bar{N}N+m\pi$ and $\bar{N}N\to\pi$'s are extensive and have been taken from the compilation from original data found in Particle Data Group, LBL Report No. LBL-58, 1972 (unpublished).

[10]G. Kalbfleisch, R. Strand, and V. Vanderburg, Phys. Lett. 29B, 259 (1969); W. A. Cooper, L. G. Hyman, W. Manner, B. Musgrave, and L. Voyvodic, Phys. Rev. Lett. 20, 1059 (1968). We are indebted to Dr. G. Kalbfleisch for discussion on the question of summing the neutral channels to obtain the zero-prong cross section.

[11]P. Astbury, G. Brautti, G. Finocchiaro, A. Michelini, D. Websdale, C. H. West, E. Polgar, W. Beusch, W. E. Fischer, B. Gobbi, and M. Pepin, Phys. Lett. 23, 160 (1966).

[12]J. Alspector, K. J. Cohen, W. C. Harrison, B. Maglich, F. Sannes, D. Van Harlingen, G. Cvijanovich, M. Matin, and J. Oostens Phys. Rev. Lett. 30, 511 (1973).

[13]See Focacci *et al.*, Ref. 1.

[14]J. Lys. Phys. Rev. 186, 1691 (1969).